Research article

Insights into the design of spray systems for cell therapies for retinal disease using computational modelling

Miriam Nweze[1,2], Tim Baker[1], G. Astrid Limb[3] and Rebecca J. Shipley[1,2,*]

[1] Department of Mechanical Engineering, University College London, UK
[2] Institute of Healthcare Engineering, University College London, UK
[3] Institute of Ophthalmology, University College London, UK

* **Correspondence:** Email: rebecca.shipley@ucl.ac.uk.

Abstract: Chronic eye diseases are the main cause of vision loss among adults. Among these, retinal degenerative diseases affect millions of people globally, causing permanent loss of cells and organ dysfunction. Despite recent progress in developing stem cell therapies for retinal diseases, methods for delivery remain an area of intense research. Aerosol technology is a promising technique with the potential to spray cells evenly and directly across the retinal surface, promoting cell attachment and survival. Here we implement mathematical modelling of the spraying process to develop organ-specific spraying parameters in this therapeutic scenario. Firstly, we characterise the rheological parameters for a typical hydrogel used for spraying cells. These parameters are then integrated into a 3D computational model of an adult human eye under realistic surgical conditions. Simulation results provide quantitative relationships between the volume flow rate of the cell-laden hydrogel, external pressure needed for aerosolization, angle of the spraying, and properties of the cell delivery. An experimental assessment is also carried out to explore the impact of spraying under the regimes identified by the computational model on cell viability. This is the first stage towards using computational models to inform the design of spray systems to deliver cell therapies onto the human retina.

Keywords: computational modelling; retina; cell-based therapy; cell spraying; cell delivery

1. Introduction

Chronic degenerative diseases affect millions of people globally [1]; they can cause permanent loss of specialised cells, often resulting in organ dysfunction and degeneration. Treatments are often palliative or aimed at delaying disease progression rather than curing the disease [2]. Organ transplantation options are limited due to a shortage of donors, together with the requirement for long-term immunosuppressive treatments for transplant patients; this motivates the development of alternative cell-based therapies. Development of stem cell technologies have received significant attention due to their potential for tissue repair whilst minimising issues associated with rejection; however there remain numerous challenges for clinical implementation, including harvesting functional cells to be therapeutically effective, as well as controlled delivery of cells to their target location [3,4].

Biomimetic cell scaffolds such as hydrogels have been developed as a vehicle for cell delivery across a range of clinical applications including neurological, gastrointestinal, orthopaedic and cardiovascular diseases [5]. Hydrogels offer a promising substrate for cell delivery as they provide a biological and mechanical environment that can be tuned to mimic the natural environment in the body, thus supporting cell function and encouraging natural repair mechanisms [6]. For numerous clinical applications, therapeutic cells need to be delivered onto a tissue surface, for example the retina [7], bladder [8], gastrointestinal surfaces [9] or skin [10]. In these settings, delivering cells seeded within a hydrogel encourages cell attachment to the host anatomical structure as well as long term cell viability [11]. Spraying of these cell-laden hydrogels has the potential for direct, controlled and rapid cell delivery to tissue surfaces [9,12].

Cell spraying was originally developed to deliver epidermal cells *in vitro* on cell culture plates, using a pump aerosol nozzle [12], and was shown to be successful in consistently delivering a spatially-uniform distribution of a cell suspension, which promoted cell proliferation after spraying[12]. This spraying technology relies on aerosolization to deliver a controlled volume of cellular hydrogel in droplet form; indeed, commercially available spraying applicators (for example, Baxter [13]) have integrated pressure regulators and nozzle adaptors to enable the volume, pressure and flow rate of the cellular scaffold to be controlled to cover a required surface area of tissue with a spatially uniform cell layer. This technology has been subsequently used both preclinically and clinically, including on animal eye models [14,15], human cutaneous wounds and ulcers [16,17] and for tracheal tissue engineering [18].

Although mechanical stress can influence cell physiology, cellular response remains challenging to quantify and knowledge of the mechanical influence of sprays on different cell types remains scarce [19]. During aerosolization, cells can be damaged by air bubbles and exposure to shear stress [19]. Some studies have explored cell viability and proliferative capacity after aerosolization, but have demonstrated high variability in cell viability (between 37 and 94% [18]). This variability is hypothesized to be due to the range of different hydrostatic, elongation and shear stress applied to the cells, as well as the environment conditions in which cells are delivered.

Control of spraying parameters is essential to achieve the optimal balance of features; for example, spraying flow rates must be high enough to induce aerosolization and guarantee sufficient cell delivery, but must also be low enough to ensure cells do not die as a consequence of the stresses they are exposed to through the spraying process [18]. There remain outstanding questions on how to tune spraying parameters to enable tissue-specific treatments. For example, currently there are no

standardised spraying conditions for delivery of cells onto a degenerated retina. Resolving these questions using physical experiments in isolation would be highly costly and time intensive, whereas integrating experimental research with computational modelling of the spraying process provides an opportunity to accelerate the process of both defining and refining spraying parameters. Here we propose this multidisciplinary approach, to provide a numerical basis for aerosolization of cell-laden hydrogels for tissue engineering applications.

We present a specific example of spraying cells onto the human retinal surface as a therapeutic option for treating retinal diseases associated with vision loss. Vision loss is a major social, medical and economic issue, affecting millions of people worldwide [20], often caused by retinal degeneration which involves progressive and irreversible loss of retinal neurons. There is a significant unmet clinical need for cell-based therapies to treat retinal diseases, and this motivates the current study. Spraying cells onto the retina offers an opportunity for controlled delivery of therapeutic cells, and here we use a computational model of the spraying process as a tool to inform the key parameters which may define selective retinal cell-based therapies.

Here we focus on a recent protocol implemented in feline eye models and under development for human application [21], consisting of complete extraction of the vitreous humour from the eye (a vitrectomy). We consider the scenario when this is followed by spraying of therapeutic cells embedded within a hydrogel directly on to the retina; the hydrogel shields the cells from mechanical stresses imparted through spraying, and the approach avoids the use of instruments which may damage the retina. Spraying of cells embedded in a scaffold has been shown to stabilise the cells during delivery and support cell survival and proliferation [3]. We simulate the retina scenario through computational modelling applied to a typical human adult eye geometry to inform spraying parameters such as the volume flow rate of cell suspension and external air pressure at the injector nozzle. In order to characterise the hydrogels and provide input parameters for the computational model, we also characterise the rheology of a fibrin-derived hydrogel used experimentally.

We present a computational model to describe spraying of cells in a geometry representative of the human eye. Model parameters are defined based on literature values as well as experiments to characterise the fibrin-derived hydrogel rheology, and the model is solved computationally using finite element methods. Furthermore, an experimental assessment of the derived parameters is used to explore cell viability post spraying, under the same conditions as the computational model. Sensitivity analyses of the model predictions demonstrate the link between key parameters (such as air pressure, volumetric flow rates) and features of the spray that must be controlled (such as retinal surface area to be covered, thickness of the cell layer, velocity of sprayed droplets). These relationships are formulated as operating equations, which enable an end-user to define spraying parameters to achieve geometry-specific outcomes. This is the first stage towards using computational models to inform the design of spray systems to deliver cell therapies onto the human retina.

2. Computational modelling and experimental methods

First of all, we present the experimental methods used to characterise the rheological properties of the hydrogels used for spraying, followed by the computational model used to describe spraying of cell-laden hydrogels in the human eye, and finally the experimental methods used to assess cell viability under different spraying conditions.

2.1. Hydrogel characterisation

We model the delivery of cells embedded in a fibrin-derived hydrogel by combining its two components, thrombin and fibrinogen [14,18]. When thrombin comes into contact with fibrinogen, it forms a fibrin gel with an insoluble matrix that can degrade *in vivo*. Here we quantify the rheological properties of fibrin-derived gels using a rheometer, in order to provide accurate parameter values for the computational model (Figure 1). These rheological properties depend strongly on the relative concentrations of thrombin and fibrinogen used to form the hydrogel. Increasing thrombin concentration relative to that of fibrinogen accelerates the gelation time, resulting in a denser gel with thinner protein fibres; however, high fibrinogen concentrations may cause clogging during spraying [22]. We therefore quantify the rheological properties of the fibrin-derived hydrogel for a range of thrombin concentrations at constant fibrinogen concentration.
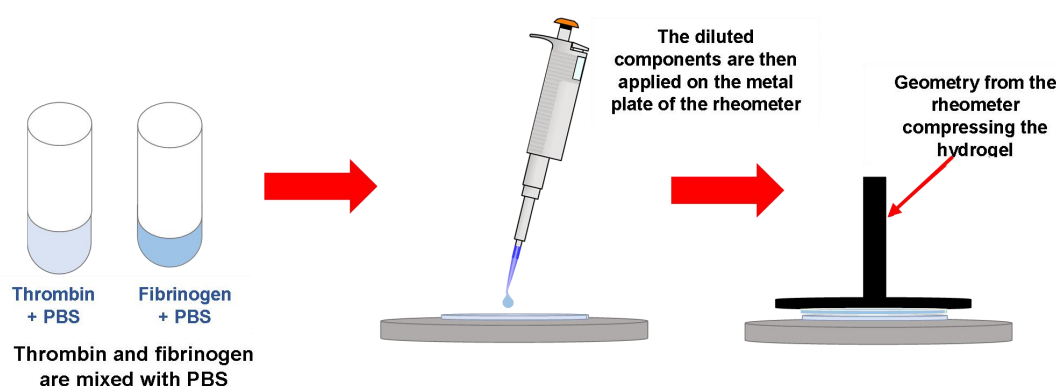

Figure 1. Thrombin and fibrinogen are diluted into PBS and mixed to produce hydrogels at a range of concentrations which then underwent rheological testing. Fibrinogen concentration was kept constant at 0.50 mg/mL, whilst thrombin was diluted from 0.30 to 0.04 U/mL.

Each component (thrombin, fibrinogen) was diluted using phosphate-buffered saline (PBS). Human thrombin (100 U/mL), purchased from Sigma-Aldrich (St Louis, USA), was diluted into 200 μL of PBS to yield concentrations from 5.00 to 0.04 U/mL. Fibrinogen (110 mg) was also diluted with 4.15 mL of PBS to achieve a final concentration of 26.50 mg/mL. Four mixtures were tested, where the concentration of fibrinogen was kept constant (0.50 mg/mL) and mixed with different thrombin concentrations; 0.30, 0.15, 0.08 and 0.04 U/mL of thrombin respectively. The samples were individually loaded onto the metal plate of the Discovery Hybrid Rheometer-3 (TA Instruments) (Figure 1), controlled at a constant temperature of 37°C. Firstly, a sweep test was carried out to evaluate different strain regimes for the hydrogel by measuring the material storage and loss moduli. The region where strain is linear, together with the corresponding shear rate value, are determined; a shear rate value of 0.015 s^{-1}was selected and applied for a flow peak hold test to determine the viscosity of the hydrogel as a function of time. For this test, hydrogel samples (with a cylinder-shaped geometry with a cross-sectional diameter of 40.0 mm and vertical height of 1.0 mm) were subject to constant shear rate of 0.015 s^{-1} for a period of 10 minutes (600 s).

2.2. Computational model

Here we outline the computational model used to describe the spraying process, as well as the underpinning parameter values and implementation. We model the spraying of a cellular suspension, comprised of stem cells embedded in fibrin-derived gel, onto the inner surface of the human retina. A two-phase spray nozzle (with the phases being air and cellular mixture) is used to generate the spray at a distance s from the sclera (Figure 2). We base the model geometry on the mean dimensions of an adult human eye, although the framework could readily be applied to individual eye geometries. In the human eye, the inner retina covers roughly three quarters of the inner optical surface [23]. The 3D modelling domain comprises a spherical eye with mean diameter of 25 mm [23], with a circular injector nozzle with an inner dimeter of 0.6 mm and positioned at (x_1, y_2, z_3) mm from the centre of the eye, which is the origin of schematic and directed to deliver cells around the optic nerve and macula.
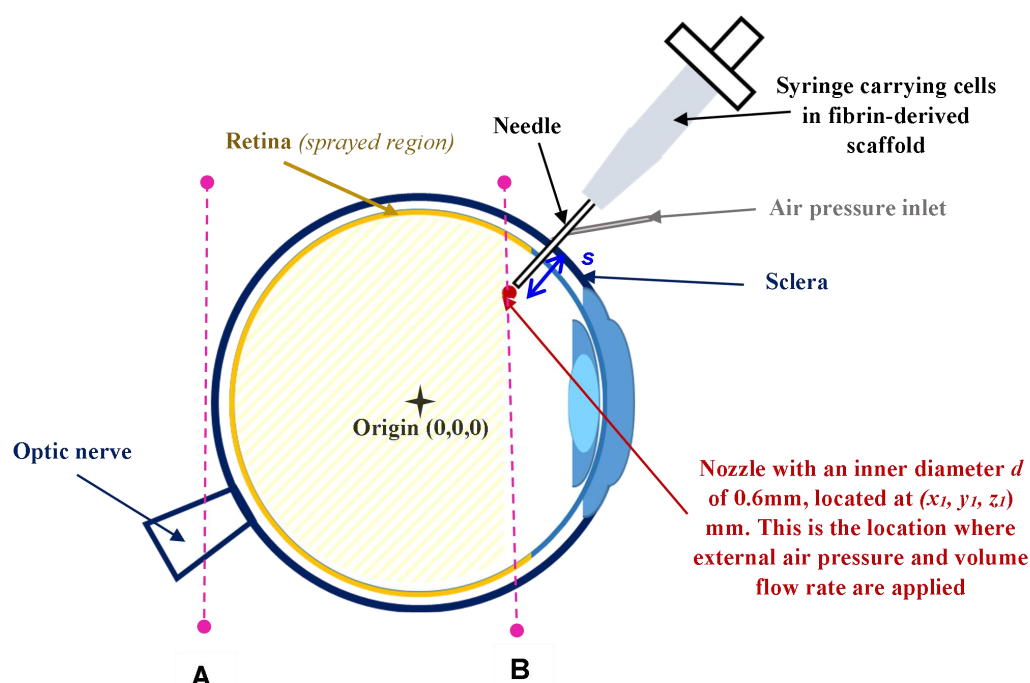

Figure 2. Schematic representation of the simulation geometry, showing the injector nozzle, optic nerve and retina locations. For the simulations presented here, the diameter of the eye (measured to the sclera) is fixed at 25 mm, the diameter to the retina is approximately 24 mm, and the injector has an inner diameter of 0.6 mm, positioned with its outlet at (x_1, y_1, z_1) mm. The position of the nozzle defines the distance s, which is the distance between the nozzle position and the sclera.

The cellular suspension is aerosolised by the injector and sprayed as droplets through the air-filled eye, directed at the optic nerve. A Lagrangian approach is adopted, with the cell suspension droplets modelled as a multiphase viscous material. The droplets' path are bounded within a cone-like region, which generates upon the fluid-gas interaction at the injector nozzle and is directed towards the optic nerve [5], and this cone-like region determines the sprayed surface area. Equations

of conservation of mass, momentum and energy would be usually solved for each phase (air and cell-laden hydrogel); however, as this is an isothermal problem, only conservation of mass and momentum are required. We assume that each phase is incompressible (i.e. constant density) and that the flow is laminar. The material properties for air (described using the Navier-Stokes equations) are well-defined, whereas the rheological parameters for the cell-laden hydrogel are determined experimentally (see section 2.1). The temperature was assumed constant at 37 °C (293 K). All parameters for the computational model are summarised in Table 1. We verify retrospectively that Reynolds number for the flow (based on the measured viscosity, typical droplet speed, and distance travelled by a droplet) is around 120, so the flow is inertia driven, but not turbulent.

Table 1. List of parameters used for the computational model. Pressures are reported as values relative to atmospheric pressure.

Parameter Description	Value
Gravitational acceleration	9.81 m/s^2
Temperature	293 K (37 °C)
Continuous phase material properties (air)	
Density	1.184 kg/m^3
Viscosity	1.855×10^{-5} Pa·s
Fibrin-derived hydrogel material properties	
Density	Determined using the material characterisation
Dynamic viscosity	experiment (see §2.1)
Duration of spraying event	1 s
Initial air pressure inside the eye	12 mmHg [24]
Injector position	(x_I, y_I, z_I) mm = (3, 7, 0) mm
Air pressure at injector	10, 25, 50, 70, 100 kPa
Volume flow rate of cellular suspension	100–400 μL/s
Outer cone angle determined by the injector	5–100°

The initial air pressure within the eye is set to a healthy intraocular pressure of 12 mmHg [6]. The pressure and volumetric flow rate of the multiphase material are imposed at the injector inlet, and varied in the ranges of 10 to 100 kPa (air pressure) and 100 to 400 μL/s to explore the impact of varying the injector parameters on distribution of cellular hydrogel [25]. No slip and flux boundary conditions are imposed on the retinal wall boundary.

The computational model described above is solved using finite element methods using the CFD solver, Simcenter STAR-CCM+®. A tetrahedral mesh was applied to the geometry and a mesh refinement study was carried out based on the film thickness predictions. Convergence was achieved at an edge element size of 0.40 mm, at which level the cell layer thickness at the retinal wall was accurate to 2 decimal places. An implicit unsteady model with segregated flow was used to solve the time-dependent conservation equations for the gas phase (the time-dependent solver comprises a second-order upwind scheme). With the aim of simulating aerosol cell-spraying and defining injector properties that will allow applying hydrogel material properties and external air pressure as a secondary inlet to create aerosolization effects, a pressure swirl injector description was used to

describe the injector inlet using the Linear Instability Sheet Atomization (LISA) model. The LISA model not only allows definition of the said parameters, This atomizer description is a primary atomization model used generically to generate small droplets distributed over a wide outer cone angle [5]. The LISA model makes the following assumptions:

- The model calculates mean droplets dimeter and droplets are generated at the injector according to the Rosin-Rammler size distribution, which describes the volume of the particles as a function of their diameter [26];
- Droplets are uniformly distributed by angle in the spray cone;
- The injector flow rate is assumed to be steady;
- The atomized particles appear at the point of injection immediately;
- The slip velocity between the fluid droplets and the surrounding air is equal to the absolute velocity of the fluid at the injector

During the atomization process, fluid droplets are sprayed from the injector in the direction of the optic nerve and move through the eye. When droplets meet the retina wall, cell attachment onto the wall is described using Bai-Gosman adhesion theory [27]. This theory (which is valid for multiphase models) models the behaviour of the cell-laden hydrogel droplets impacting on the retinal wall by predicting how and when break up takes place. Although its application to these hydrogels and spraying protocols have not been tested, it is a logical starting point for building a computational model of the spraying process. The hydrogel within the injector is subject to centrifugal motion, generating a liquid film surrounding an air cone. The thickness and velocity of the hydrogel subject to the centrifugal motion are calculated based on input parameters at the injector. The initial hydrogel thickness in the nozzle, δ_0, is determined via

$$\dot{m}_f = \pi \rho u_f \delta_0 (d_0 - \delta_o), \tag{1}$$

Where $\dot{m}_f$ is the hydrogel mass flow rate at the injector, ρ is the air density, d_0 is the injector diameter and u_f the axial component of the velocity at the injector. Firstly, a swirling motion applies as the air pressure is applied at the injector nozzle, gradually forming a film of the injected liquid with initial thickness δ_o within the injector. As the liquid starts to accelerate, it then creates a sheet breakup, ultimately undergoing atomization. We use this relationship in the LISA model to predict the ejection of the cell-laden hydrogel from the injector into the eye cavity. This is the first time these models have been used to predict spraying processes in the eye, and they will require extensive validation to be taken forward; however, this model serves as a natural starting point given the extensive use of the approach to describe spraying of a range of materials across extensive application areas.

2.3. Experimental assessment of spraying parameters

Experiments were carried out to assess the impact of different spraying conditions (volume flow rate, nozzle pressure) on cell viability.

2.3.1. Cell culture

Müller stem cells (cell line MIO-M1 previously reported in [28]) were passaged by creating monolayers of cultured cells and dissociated using 3 mL of TrypeIE ™ 1× (Life technologies), and incubated for 5 minutes at 37 °C, with 5% CO_2. Cells were culuresd in a flask containing Dulbecco's Modified Eagle Medium (DMEM) ×1 with GlutaMAX with 10% Foetal Calf Bovine Serum (FCS) (Invitrogen, UK) and Penicillin/Streptomycin (10000 units per 5 mL in the T-25 flask).Cell suspensions were centrifuged at 1400 rpm for 5 minutes at 15 °C.

Cells stock was maintained through cryopreservation of cultured cells and performed by re-suspending cell pallets from T-25 culture flask in 1 mL of freezing mix made from 40% FCS and 10% Dimethyl Sulfoxide (DMSO) (Sigma-Aldrich, UK) in DMEM. The cellular suspension was transferred to cryovials placed in an isopropanol freezing cassette at −80 °C for 24 hours. This was performed to ensure controlled cryopreservation. The frozen suspension was then transferred to −150 °C for longer storage. Cells were grown and passaged in DMEM containing L-Glutamax without pyruvate (PAA, UK), 10% FCS (Biosera) 5 mL of Penicillin (2,000 U/mL) combined with streptomycin (2,000 μ/mL) (Life Technologies) in 500 mL of DMEM. Cells were incubated at 37 °C in 5% CO_2, air atmosphere.

2.3.2. Cell spraying

After culturing the cells, the thrombin and PBS combined with the MIO-M1 cells are loaded separately from the fibrinogen, which was also diluted into PBS (150 μL of thrombin mixed with 1.17 mL of PBS, hence giving a total volume of 1.32 mL). The Baxter spray system was connected to the external pressure regulator, where the injector pressure was applied (50, 70 and 100 kPa). The spray system is intended for spraying cells that can attach to the retina, such as Müller glial cells. Müller glia are structurally supportive cells, have a very high metabolic function and are very resilient to stress. Neurons are very sensitive to physical and metabolic damage and the spray is not intended for use with neurons. The cell laden hydrogel was sprayed onto a 6-well plate at a distance of 2 cm from nozzle to the sprayed surface, with a volume flow rate of 400 μL/s. Temperature was maintained at 37 °C.

Once sprayed, the cell-laden hydrogel was stained with trypan blue, to assess cell viability of MIO-M1 cells post-aerosolization. Experiments were conducted to assess surface areas post-aerosolization by spraying the fibrin-derived hydrogel, oil and water at pressure of 50, 70 and 100 kPa respectively. Each fluid was stained with trypan blue and sprayed onto filtered paper in a petri dish.

3. Results

3.1. Rheology of fibrin-based hydrogels

Figure 3 describes how the viscosity of the hydrogel varies in time for fibrin-derived mixtures with different thrombin concentrations. The fibrinogen concentration is kept constant for all the hydrogel mixtures (0.50 mg/mL). When subject to constant shear, the viscosity of the fibrin-based hydrogel increases as a function of time and then equilibrates, showing an increase in structural strength of the tested samples between 1 and 5 s. The lower the concentration of thrombin, the

slower the rate to reach the same viscosity of a higher thrombin concentration. For example, for the diluted sample with 1.00 µL of thrombin (0.30 U/mL), the viscosity increases between 3 and 9 Pa.s in just over 2 s. On the other hand, the sample with 0.25 µL of thrombin (0.08 U/mL) takes double the time to achieve the same viscosity. The relationship from Figure 3 shows the viscosity increases in time across all samples; the higher the thrombin concentration, the higher the gel viscosity. The relaxation time for the hydrogel samples is beyond the 5 s timescale of our experiments. The dynamic viscosity gradient in time was also dependent on the thrombin concentration; the higher the thrombin concentration, the denser the gel and the higher the maximum linear viscosity before reaching the relaxation period. Thus, the lower the concentration of thrombin in the hydrogel, the longer it takes for the sample to increase in viscosity. We select the mixture with 0.25 µL of thrombin (0.08 U/mL) and total volume of 100 mL and input its time-dependent viscosity into the computational model based on interpolating the data provided in Figure 3. We note that the time taken for spraying is only 1 second, so the viscosity is approximately constant during this time. However, we note that it would be straightforward to use the computational model to explore other viscosity profiles in future.
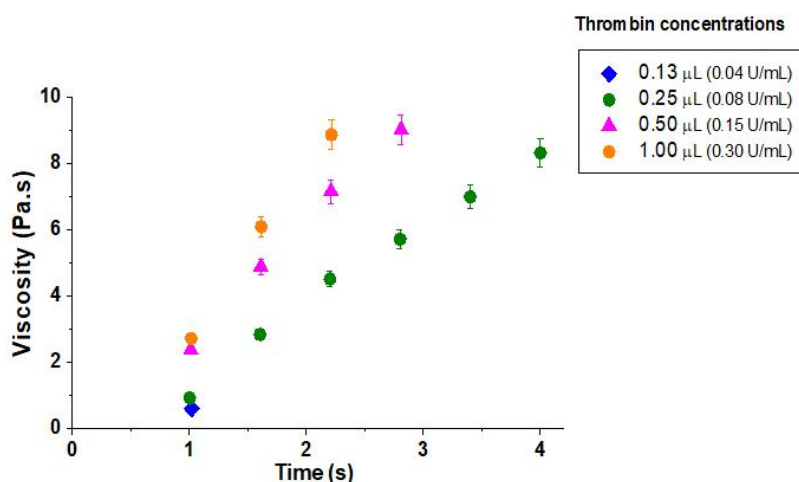

Figure 3. Dynamic viscosity as a function of time for fibrin-based hydrogels with constant fibrinogen concentration (0.50 mg/mL) and a range of thrombin concentrations (results show mean viscosity with error bars representing the standard deviation based on n = 3 repeats). In general, higher thrombin concentrations yielded hydrogels with a higher viscosity. The time-dependent viscosity relationships determined here were inputted into the computational model to predict spraying properties based on the gel being formed instantaneously when the aerosolisation begins.

3.2. Predictions of the computational model

Here we use the computational model described in section 2.2 to explore the impact of varying the pressure and volume flow rate of cell-laden hydrogel at the injector nozzle, as well as the outer cone angle for the spray, on a number of key outputs of high priority in terms of control of the spraying process:
  (i) Properties of the layer of cell-laden hydrogel on the retinal wall;

(ii) Surface area of the retina covered;

(iii) Droplets' speed and wall shear stress on the retinal surface.

This spraying system is intended for spraying cells onto the inner limiting membrane of the retina. The protein nature of the gel protects the cells being sprayed, and the inner limiting membrane, which is composed of extracellular matrix proteins, forms a barrier that protects inner retinal neurons from external insult. We explore volume flow rates at the injector ranging between 100 to 400 µL/s, respectively, and injector pressures of 10 to 100 kPa above atmospheric. The pressure applied is much lower than that recommended by spray system manufacturers to spread fibrinogen gels and cells onto the diseased skin and gut, because of the relative size of the eye, and volume of cells that need to be delivered [16].

3.2.1. Properties of the cell-laden hydrogel layer sprayed onto the retinal surface

The thickness of the cell-laden hydrogel sprayed on the retinal surface was examined at varying flow rates (from 150 to 275 µLs^{-1}) with the inlet pressure fixed at 10 kPa, and cone angle fixed at 50° (Figure 4). The thickness of the retinal hydrogel layer (subsequently referred to as film thickness) is broadly uniform, consistent with a literature investigation [18,29], and this layer thickness increases with increased volume flow rates, as expected.
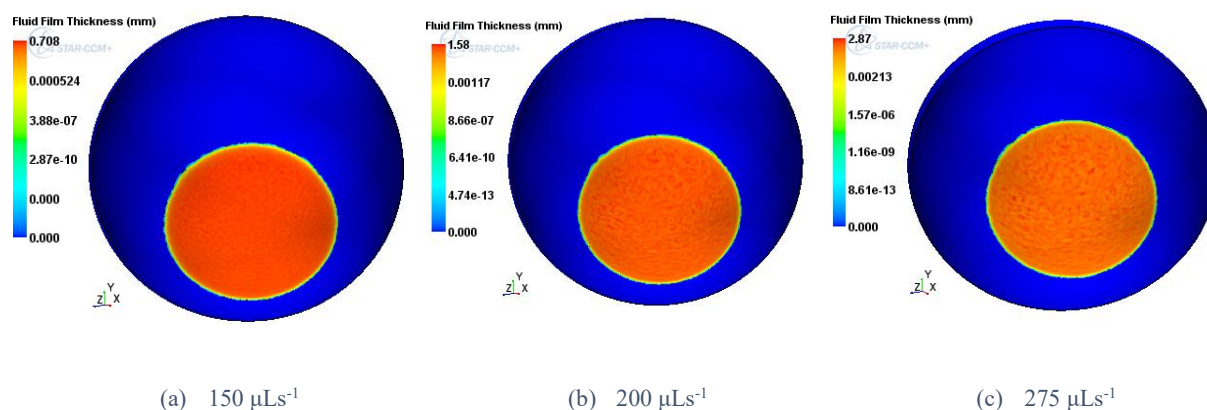

(a) 150 µLs^{-1} (b) 200 µLs^{-1} (c) 275 µLs^{-1}

Figure 4. Logarithmic scale of fluid film thickness distribution on the retina, with varying volume flow rate between 150 to 275 µL_s^{-1}, at a constant pressure condition of 10 kPa at the injector and subject to an outer cone angle of 50°.

Figure 5 shows the relationship between maximum fluid film thickness and volume flow rate at the injector, for varying injector pressures. The maximum fluid film thickness increases non-linearly with the injector volume flow rate at given pressures; for a fixed injector volume flow rate, increasing injector pressure also increases the maximum film thickness. The data presented in Figure 5 were fitted to an exponential relationship of the form $y = Ae^{Bx}$, where y is the maximum thickness of the fluid film, x is the volumetric flow rate at the injector, and A, B are constants which are determined by regression analysis for each injector pressure condition. This yields operating equations which describe maximum film thickness as a function of injector volume flow rate at different injector pressures. These relationships enable a desired thickness on the retina to be

achieved by selecting the injector volume flow rate used. For example, the exponential relationship between maximum film thickness (y) and volume flow rate (x) at 10 kPa is $y = 0.30e^{0.004x}$ (Figure 5 and Table 2). To achieve a film thickness of 1.5 mm using an injector pressure of 10 kPa and applying an outer cone angle of 50°, inverting this equation indicates the cellular suspension should be sprayed at 400 μLs^{-1}.
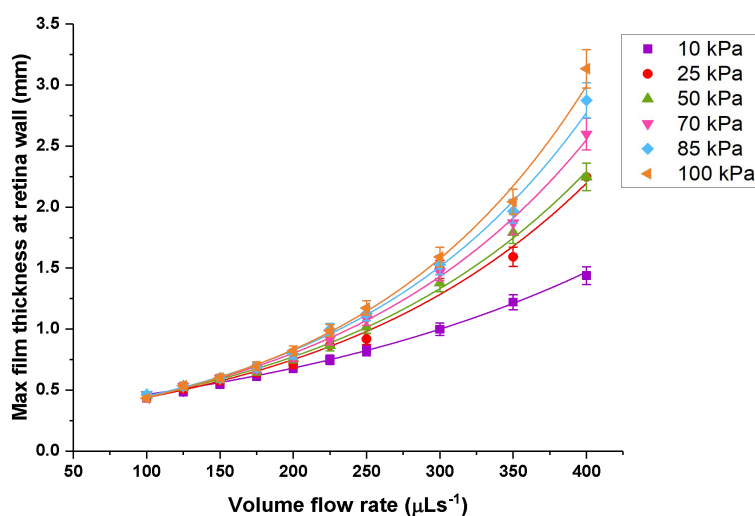

Figure 5. The maximum film thickness at the retina surface (y-axis) has an exponential relationship with the volume flow rate (x-axis), for each given pressure value and at an outer cone angle of 50°. Data points show the mean, and error bars +/−1 standard deviation from the mean, when averaging across the spatial domain. Lines show fitted exponential relationship based on defined relationships in Table 2, with R^2 values quantifying the fit between each regression line and corresponding data points (ranging between 0.91 and 0.98) summarised in Table 2.

Table 2. Exponential relationships linking maximum film thickness (mm, y) with volume flow rate (μL/s, x), at different inlet pressures, as summarised in Figure 5. R^2 values quantify the fit between each exponential relationship and the corresponding data points (Figure 5).

Pressure/ kPa	Equation	R^2
10	$y = 0.30e^{0.004x}$	0.98
25	$y = 0.26e^{0.0054x}$	0.93
50	$y = 0.26e^{0.0054x}$	0.95
70	$y = 0.25e^{0.0058x}$	0.94
85	$y = 0.24e^{0.0061x}$	0.92
100	$y = 0.23e^{0.0064x}$	0.91

3.2.2. Surface area of the retina covered

The surface area of the retinal surface covered is dependent on the cone angle of the spray at the injector (Figure 6a). Our results indicate an exponential relationship between the covered surface area of the inner retina and the outer cone angle of the spray, for fixed injector volume flow rate and pressure (Figure 6b), specifically the surface area (y) is related to the outer cone angle (x) via $y = e^{C+Dx+Ex^2}$, where C, D, E are constants that are determined for each injector volumetric flowrate and pressure combination. The exponential relationships identified in Figure 6b are $y = e^{(2.60+0.074x-3.51x^2)}$ at 25 kPa and $y = e^{(3.15+0.064x-3.10x^2)}$ at 100 kPa. Through these relationships, the outer cone angle can be used to control the surface area of the retina covered through spraying. The increased pressure at the injector does not significantly affect the surface area covered, as this is specified through outer cone angle values (Figure 6b).
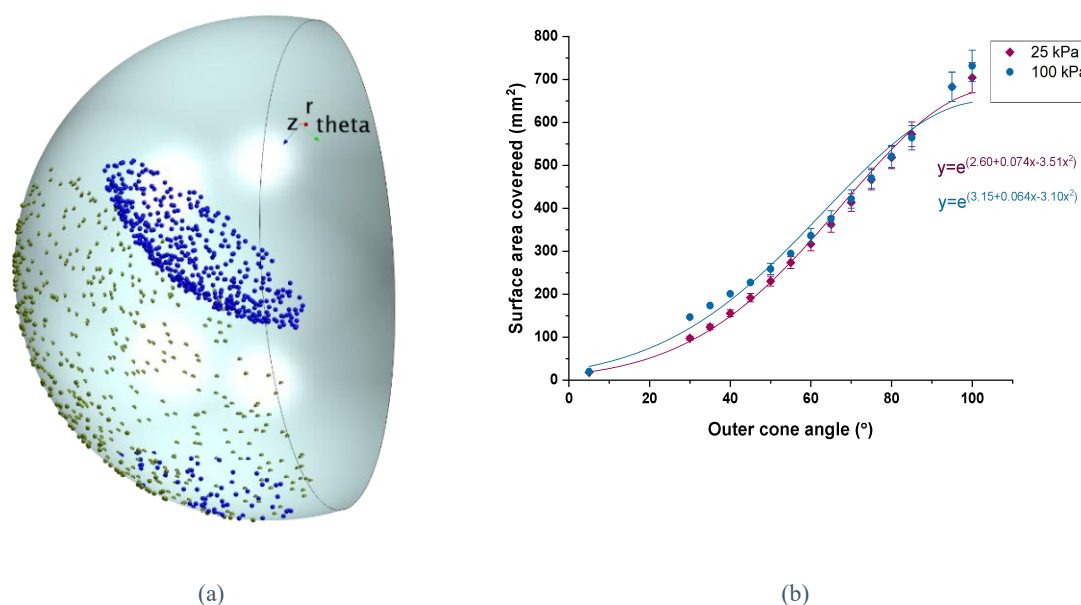

(a)   (b)

Figure 6. (a) A schematic of the 3D eye model including the spatial and temporal distribution of sprayed droplets. The z-axis represents the direction of the trajectory of the sprayed droplets (i.e. the straight-line direction from the injector to the optic nerve). (b) Relationship between surface area of the retina covered and outer cone angle of the spray at the injector (varying between 5° to 100°), using volume flow rate of 250 μL/s at 25 kPa and 400 μL/s at 100 kPa. Data points indicate means and error bars +/−1 standard deviation of the mean, averaged over the spatial domain.

3.2.3. Droplets' speed and wall shear stress on the retinal surface

Finally, the impact of varying injector pressure, volumetric flow rate and cone angle of spraying on the speed of sprayed droplets, and shear stress on impact with the retinal wall. We note that both shear and normal stresses will be communicated to the cell population and will influence

cell fate. The computational framework can explore both; however, we focus on shear stress here to demonstrate the behaviour of the model. Droplets' speed is compared for different pressure conditions at the injector nozzle, for a constant volume flow rate and outer cone angle (Figure 7a), with an increase in mean droplet speed with increasing pressure at the injector observed over the range tested.
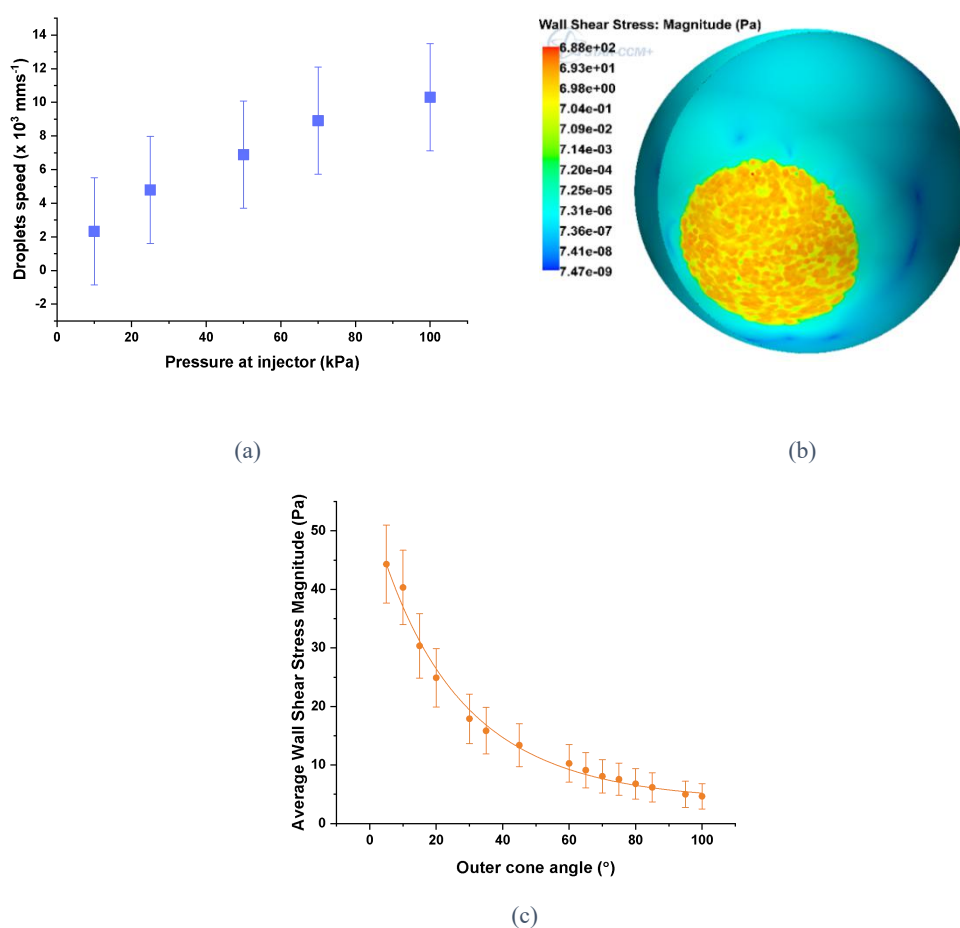

(a)

(b)

(c)

Figure 7. (a) Mean and variability in droplet speed on the retinal surface for varying injector pressure (volume flow rate and outer cone angle held fixed at 400 µL/s, 50° respectively; error bars $+/-2$ standard deviations from the mean). (b) The predicted spatial distribution of the shear stress on the retinal surface, for a volume flow rate of 200 μLs^{-1} and pressure of 70 kPa. (c) Average wall shear stress magnitude on the retinal wall, for varying outer cone angles (5 to 100°), with volumetric flow rate and injector pressure held fixed at 400 µL/s and 100 kPa respectively (error bars representing standard $+/-1$ standard deviations from the mean).

Figure 7b provides a visualisation of the corresponding spatial distribution of shear stress magnitude when the sprayed cells impact on the retinal wall, with average wall shear stress plotted as a function of outer cone angle of the spray at the injector in Figure 7c. As this outer cone angle is increased, the average wall shear stress decreases non-linearly due to dissipation of the spray momentum across a larger surface area of the retinal wall. The exposure of cells to shear stresses

(both during spraying and upon impact on the retinal wall) may induce cell death, and the relationships in Figure 7 provide information on how to mitigate for this, based on tuning the spraying parameters (injector pressure, volume flow rate, spray outer cone angle). Furthermore, with these prediction and derived parameters for the biomaterial, we predict the flow to have a Reynold's number of 15.4 at a pressure of 50 kPa
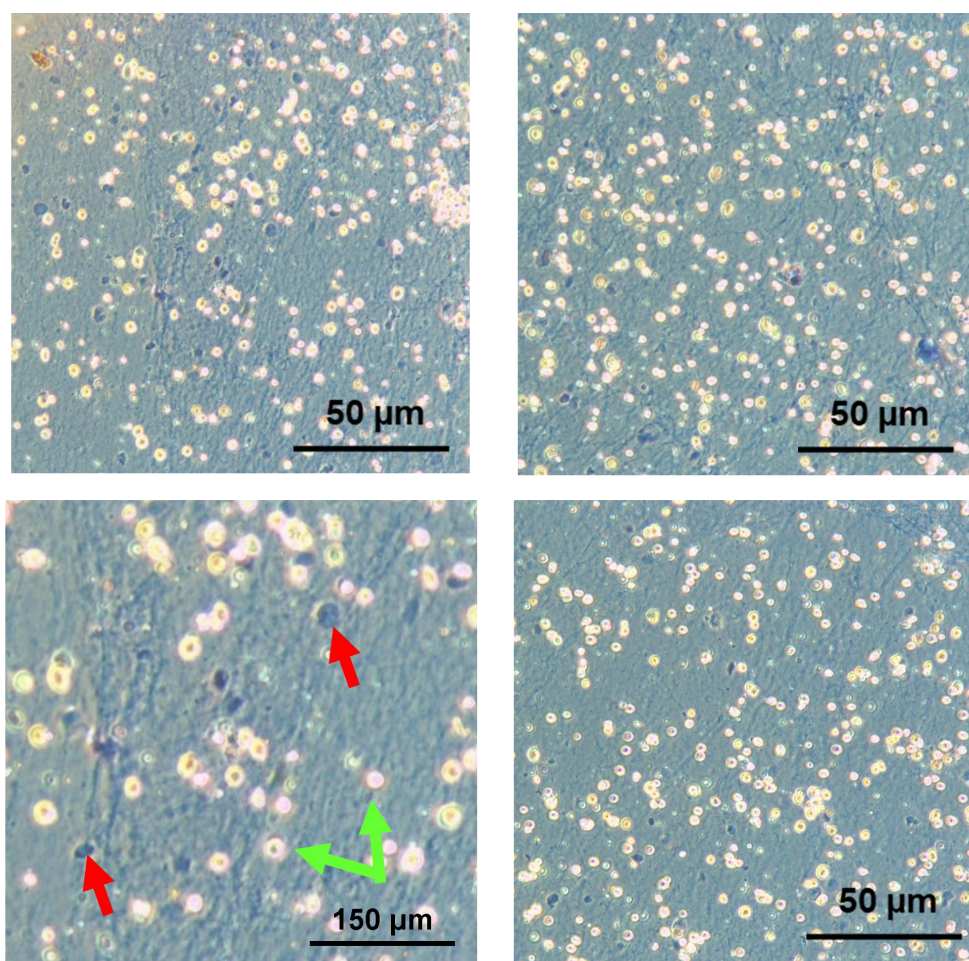

Figure 8. Viability of Müller stem cells sprayed with the Baxter Healthcare Easyspray system at pressure of 100 kPa using trypan blue staining using a Leica TCS-SP2 confocal microscope at 20× magnification. Images were processed through Leica AF Lite Confocal Software and ImageJ for further analyses. After being cultured, cells are mixed with the fibrin-derived hydrogel (with a thrombin concentration of 0.08 U/mL) and sprayed at a volume flow rate of 400 µL/s on a 6-well plate and applying an external pressure of 100 kPa and the second inlet of the spraying device. The sprayed cell laden-hydrogel is then coated with 50 µL trypan blue, diluted into 200 µL of PBS. The red arrows indicate the dead cells and the green arrows the live cells (scale of 50 µm). The experiment was repeated three times.

3.3. Experimental assessment of spraying parameters

3.3.1.   Cell viability

Collectively, these data show a high rate of survival for the sprayed Müeller stem cells, within this pressure range (Figures 8–10). The results indicate that, within the range tested, higher pressures gave rise to higher cell viability (Figure 11). There are numerous mechanisms which could give rise to this trend, for example the cells may respond positively to shear stimulation, or the increased pressures may increase the probability of attachment to the surface upon spraying.
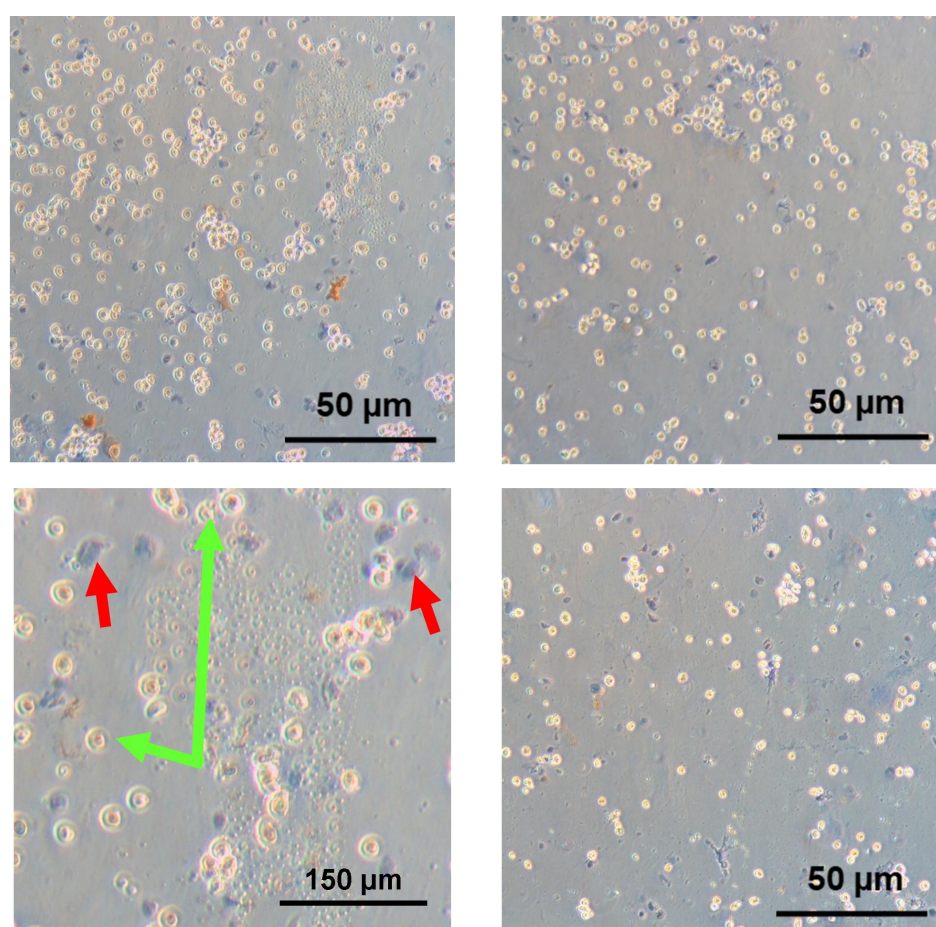

Figure 9. Viability of Müller stem cells sprayed with the Baxter Healthcare Easyspray system at pressure of 70 kPa using trypan blue staining using a Leica TCS-SP2 confocal microscope at 20× magnification. Images were processed through Leica AF Lite Confocal Software and ImageJ for further analyses. After being cultured, cells are collected using fibrin-derived hydrogel (with a thrombin concentration of 0.08 U/mL) and sprayed at a volume flow rate of 400 µL/s on a 6-well plate and applying an external pressure of 70 kPa and the second inlet of the spraying device. The sprayed cell laden-hydrogel is then coated with 50 µL trypan blue, diluted into 200 µL of PBS. The red arrows indicate the dead ells and the green arrows the live cells. Images were taken at 20× magnification. The experiment was repeated three times.
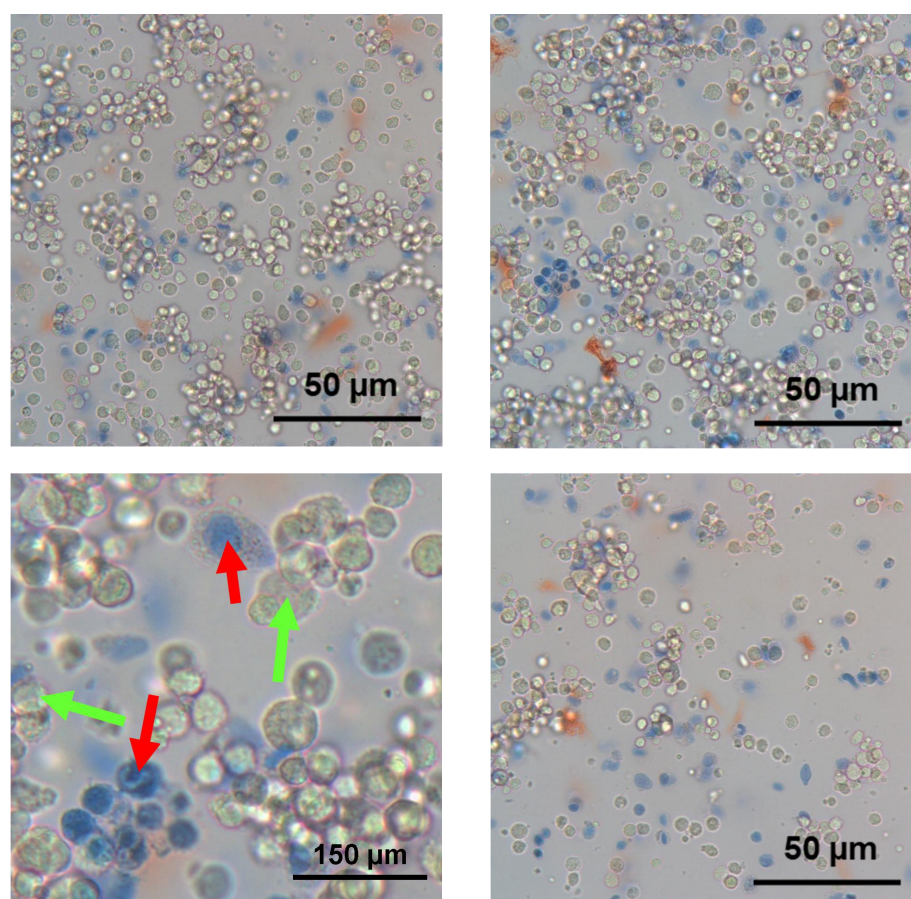
Figure 10. Viability of Müller stem cells sprayed with the Baxter Healthcare Easyspray system at pressure of 50 kPa using trypan blue staining using a Leica TCS-SP2 confocal microscope at 20× magnification. Images were processed through Leica AF Lite Confocal Software and ImageJ for further analyses. After being cultured, cells are collected using fibrin-derived hydrogel (with a thrombin concentration of 0.08 U/mL) and sprayed at a volume flow rate of 400 µL/s on a 6-well plate and applying an external pressure of 50 kPa and the second inlet of the spraying device. The sprayed cell laden-hydrogel is then coated with 50 µL trypan blue, diluted into 200 µL of PBS. The red arrows indicate the dead ells and the green arrows the live cells. Images were taken at 20× magnification. The experiment was repeated three times.

4. Conclusion

This work uses computational modelling as a tool to explore spraying parameters for cell-laden hydrogels for retinal damage repair. Specially, computational models of hydrogel spraying are used to explore the impact of varying spraying parameters (pressure and volume flow rate at the injector nozzle, outer cone angle for the spray) on key outputs of high priority, namely the spatial distribution of the delivered hydrogel on the retinal wall, the surface area of the retina covered, and droplet speed.
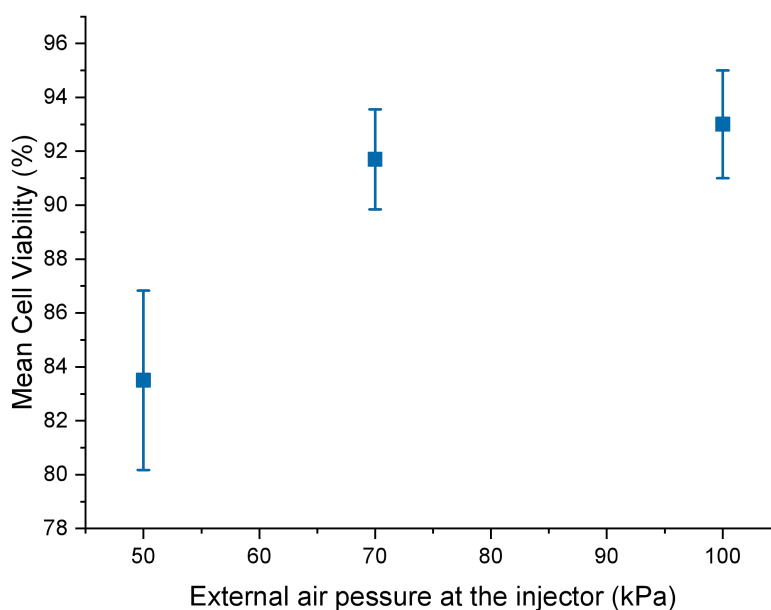
Figure 11. The mean cell viability of the sprayed Müller stem cell lines MIO-M1 with the pressure at the injector (x-axis) sprayed at a volume flow rate of 400 µL/s on a 6-well plate with the fibrin-derived hydrogel, with constant fibrinogen concentration (0.5 mg/mL). Data points show the mean cell viability, with error bars representing the standard deviation based on n = 3 repeats ($p < 0.38$).

This is the first time that a computational model has been developed and applied to explore spraying parameters for cell-laden hydrogels in the eye, and there are numerous opportunities for further extension and validation. First of all, the computational models applied here have been used extensively in a range of applications, but have not been validated for the current application. We include an experimental assessment of the rheological properties of the hydrogel, and also cell viability post spraying. There is opportunity to expand the study of these variables, for example to characterise the link between hydrogel viscosity and seeded sell density. Numerous spraying parameters require validation (for example, droplet size, outer cone angle, and properties of the hydrogel layer delivered to the retinal surface), and this will require extensive further experimental work, including in animal models. Based on the results of this process, there is the opportunity to fine tune the parameters and relationships used in the computational spraying model. Further experimental work to explore how exposure to mechanical stress influences cell viability who enable more concrete relationships to be built to predict the impact of spraying parameters on cell outcomes.

The approach presented here provides a first step towards the use of computational models to inform the design of spray systems to deliver cell therapies to the retina. The approach will require extensive experimental validation, but provides an interdisciplinary approach to both gain insight into, and inform, spraying processes for cell delivery.

Acknowledgments

Conflict of interest

There are no conflicts of interest to disclose.

References

1. WHO. Chronic Diseases and Health Promotion, World Health Organisation, 2017. Available from: http://www.who.int/chp/en/.

2. R. E. Maclaren, R. A. Pearson, A. Macneil, R. H. Douglas, T. E. Salt, M. Akimoto, et al., Retinal repair by transplantation of photoreceptor precursors, *Nature*, **444** (2006), 203–207.

3. M. H. Amer, F. R. A. J. Rose, K. M. Shakesheff, M. Modo, L. J. White, Translational considerations in injectable cell-based therapeutics for neurological applications: Concepts, progress and challenges, *npj Regen. Med.*, **2** (2017), 23.

4. J. Steinbeck, L. Studer, Moving stem cells to the clinic: Potential and limitations for brain repair. *HHS Public Access*, **86** (2015), 1922–2013.

5. D. P. Schmidt, I. Nouar, P. K. Senecal, J. Rutland, J. K. Martin, R. D. Reitz, et al., Pressure-swirl atomization in the near field, *SAE Trans.*, **108** (1999), 471–484.

6. H. C. Geijssen, *Studies on Normal Pressure Glaucoma*, Kugler Publications, 1991.

7. S. Singhal, B. Bhatia, H. Jayaram, S. Becker, M. F. Jones, P. B. Cottrill, et al., Human muller glia with stem cell characteristics differentiate into retinal ganglion cell (RGC) precursors *in vitro* and partially restore RGC function *in vivo* following transplantation, *Stem Cells Transl. Med.*, **1** (2012), 188–99.

8. A. T. Hafez, D. J. Bagli, A. Bahoric, K. Aitken, C. R. Smith, D. Herz, et al., Aerosol transfer of bladder urothelial and smooth muscle cells onto demucosalized colonic segments: A pilot study, *J. Urol.*, **169** (2003), 2316–2320.

9. A. Roberts, B. E. Wyslouzil, L. Bonassar, Aerosol delivery of mammalian cells for tissue engineering, *Biotechnol. Bioeng.*, **91** (2005), 801–807.

10. M. Cohen, A. Bahoric, H. M. Clarke, Aerosolization of epidermal cells with fibrin glue for the epithelialization of porcine wounds with unfavorable topography, *Plast. Reconstr. Surg.*, **107** (2001), 1208–1215.

11. A. A. Foster, L. M. Marquardt, S. C. Heilshorn, The diverse roles of hydrogel mechanics in injectable stem cell transplantation, *Curr. Opin. Chem. Eng.*, **15** (2017), 15–23.

12. A. Bahoric, A. R. Harrop, H. M. Clarke, R. M. Zuker, Aerosol vehicle for delivery of epidermal cells—An *in vitro* study, *Can. J. Plast. Surg.*, **5** (1997), 153–156.

13. G. Marx, Evolution of fibrin glue applicators, *Transfus. Med. Rev.*, **17** (2003), 287–298.

14. S. S. Chaurasia, R. Champakalakshmi, R. I. Angunawela, D. T. Tan, J. S. Mehta, Optimization of fibrin glue spray systems for ophthalmic surgery, *Transl. Vis. Sci. Technol.*, **1** (2012), 2.

15. H. Jayaram, S. Becker, K. Eastlake, M. F. Jones, D. G. Charteri, G. A. Limb, Optimized feline vitrectomy technique for therapeutic stem cell delivery to the inner retina, *Vet. Ophthalmol.*, **17** (2014), 300–304.

16. V. Falanga, S. Iwamot, M. Chartier, T. Yufit, J. Butmarc, N. Kouttab, et al., Autologous bone marrow–derived cultured mesenchymal stem cells delivered in a fibrin spray accelerate healing in murine and human cutaneous wounds, *Tissue Eng.*, **13** (2007), 1299–1312.

17. R. S. Kirsner, W. A. Marston, R. J. Snyder, T. D. Lee, D. I. Cargill, H. B. Slade, Spray-applied cell therapy with human allogeneic fi broblasts and keratinocytes for the treatment of chronic venous leg ulcers: A phase 2, multicentre, double-blind, randomised, placebo-controlled trial, *Lance*, **380** (2012), 977–985.

18. A. L. Thiebes, S. Albers, C. Klopsch, S. Jockenhoevel, C. G. Cornelissen, Spraying respiratory epithelial cells to coat tissue-engineered constructs, *Bio. Res. Open Access*, **4** (2015), 278–287.

19. I. Abu-Reesh, F. Kargi, Biological responses of hybridoma cells to defined hydrodynamic shear stress, *J. Biotechnol.*, **9** (1989), 167–178.

20. A. Hamon, J. E. Roger, X. J. Yang, M. Perron, Müller glial cell-dependent regeneration of the neural retina: An overview across vertebrate model systems, *Dev. Dyn.* **245** (2016), 727–738.

21. S. Becker, H. Jayaram, G. A. Limb, Recent advances towards the clinical application of stem cells for retinal regeneration, *Cells*, **1** (2012), 851–873.

22. Y. Li, H. Meng, Y. Liu, B. P. Lee, Fibrin gel as an injectable biodegradable scaffold and cell carrier for tissue engineering, *Sci. World J.*, **2015** (2015), 685690.

23. H. Gross, F. Blechinger, B. Achnter, Human eye, in *Handbook of Optical Systems*, WILEY-VCH, (2008), 3–20.

24. J. Flammer, S. Orgül, Optic nerve blood-flow abnormalities in glaucoma, *Prog. Retin. Eye Res.*, **17** (1998), 267–289.

25. K. Dijkstra, J. Hendriks, M. Karperien, L. A. Vonk, D. B. E. Saris, Arthroscopic airbrush-assisted cell spraying for cartilage repair: Design, development, and characterization of custom-made arthroscopic spray nozzles, *Tissue Eng. Part C Methods*, **23** (2017), 505–515.

26. A. H. Lefebvre, V. G. McDonell, *Atomization and Sprays*, (ed. N. Chigier), 2nd edition, Boca Raton: Taylor & Francis Group, CRC Press, 2017, 1–13.

27. C. X. Bai, H. Rusche, A. D. Gosman, Modelling of gasoline spray impingement, *Atomization Sprays*, **12** (2002), 1–27.

28. J. M. Lawrence, S. Singhal, B. Bhatia, D. J. Keegan, T. A. Reh, P. J. Luthert, et al,. MIO-M1 cells and similar müller glial cell Lines derived from adult human retina exhibit neural stem cell characteristics, *Stem Cells*, **25** (2007), 2033–2043.

29. A. T. HAFEZ, K. AFSHAR, D. J. BÄGLI, A. Bahoric, K. Aitken, C. R. Smith, et al., Aerosol transfer of bladder urothelial and smooth muscle cells onto demucosalized colonic segments for porcine bladder augmentation *in vivo*: A 6 week experimental study, *J. Urol.*, **174** (2005), 1663–1668.